AD_____

Award Number: W81XWH-04-1-0673

TITLE: Mitotic Spindle Directed Therapeutics for Early Stage Breast Carcinoma

PRINCIPAL INVESTIGATOR: Sucharita J. Mistry, M.D.

CONTRACTING ORGANIZATION: Mount Sinai Medical Center
New York, NY 10029-6574

REPORT DATE: September 2005

TYPE OF REPORT: Final

PREPARED FOR: U.S. Army Medical Research and Materiel Command
Fort Detrick, Maryland 21702-5012

REPORT DOCUMENTATION PAGE

Form Approved
OMB No. 0704-0188

1. REPORT DATE *(DD-MM-YYYY)*	2. REPORT TYPE	3. DATES COVERED *(From - To)*
01-09-2005	Final	31 Aug 2004 – 30 Aug 2005

4. TITLE AND SUBTITLE
Mitotic Spindle Directed Therapeutics for Early Stage Breast Carcinoma

5a. CONTRACT NUMBER

5b. GRANT NUMBER
W81XWH-04-1-0673

5c. PROGRAM ELEMENT NUMBER

6. AUTHOR(S)
Sucharita J. Mistry, M.D.

E-Mail: sucharita.mistry@mssm.edu

5d. PROJECT NUMBER

5e. TASK NUMBER

5f. WORK UNIT NUMBER

7. PERFORMING ORGANIZATION NAME(S) AND ADDRESS(ES)

Mount Sinai Medical Center
New York, NY 10029-6574

8. PERFORMING ORGANIZATION REPORT NUMBER

9. SPONSORING / MONITORING AGENCY NAME(S) AND ADDRESS(ES)
U.S. Army Medical Research and Materiel Command
Fort Detrick, Maryland 21702-5012

10. SPONSOR/MONITOR'S ACRONYM(S)

11. SPONSOR/MONITOR'S REPORT NUMBER(S)

12. DISTRIBUTION / AVAILABILITY STATEMENT
Approved for Public Release; Distribution Unlimited

13. SUPPLEMENTARY NOTES

14. ABSTRACT

Abstract # P46, Era of Hope, Breast cancer research meeting, 2005

15. SUBJECT TERMS
No Subject Terms Provided

16. SECURITY CLASSIFICATION OF:			17. LIMITATION OF ABSTRACT	18. NUMBER OF PAGES	19a. NAME OF RESPONSIBLE PERSON
a. REPORT	b. ABSTRACT	c. THIS PAGE			USAMRMC
U	U	U	UU	10	19b. TELEPHONE NUMBER *(include area code)*

For the proposed studies, we used a recombinant adenovirus that carries anti-stathmin ribozyme, Rz184, for inhibiting stathmin expression in breast cancer cells. We used a bicistronic expression vector, pAdCMV5-IRES-GFP, that contains an adenovirus origin of replication and 2.5 kilobases of human adenovirus type 5 (Ad5) DNA for efficient homologous recombination. This vector also contains an internal ribosome entry site (IRES) element derived from the encephalomyocarditis virus that permits the translation of two open reading frames from the same messenger RNA. The IRES expression cassette of this vector is downstream from a unique cloning site to allow co-expression of a green fluorescent protein (GFP) selectable marker and the therapeutic gene i.e. the ribozyme. Both the selectable and the therapeutic gene are placed under the control of CMV5, a CMV promoter-enhancer modified for maximal expression. This arrangement allows high-level expression of the transgene and easy visualization and/or selection of transduced cells. We also generated a control adenovirus that carries GFP but not the ribozyme. The schematic illustrations of the adenoviral vectors are shown in Fig.1. We tested the activity of these recombinant adenoviruses in JC and SC115 *in vitro* murine models of breast cancer.

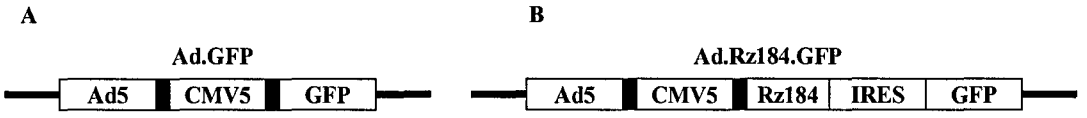

Fig.1 Schematic illustrations of the adenoviral vectors Ad.GFP (A) and Ad.Rz184.GFP (B). The control Ad.GFP adenovirus contains the GFP gene alone placed under the control of CMV5 promoter. The anti-stathmin adenovirus Ad.Rz184.GFP contain the Rz184 ribozyme encoding gene, IRES and the GFP gene under the control of a CMV5 promoter

The efficiency of adenovirus infection was assessed by infecting the cells with anti-stathmin adenovirus at increasing moi. As controls, the cells were either mock infected or infected with the control Ad.GFP adenovirus at a similar moi to determine if adenoviral infection results in cytotoxicity. The efficiency of gene transfer was determined by quantifying the fraction of cells that expressed GFP by flow cytometry. Infection of cells with control or anti-stathmin adenovirus at increasing moi's from 25 to 200 resulted in a progressive increase in the percentage of transduced cells. The optimal moi for SC115 and JC cells was determined to be in the range of 25-100 and 50-200 respectively. Infection at these moi's resulted in efficient transduction without any significant cytotoxicity.

Effect of anti-stathmin ribozyme on stathmin expression in breast cancer cells:
We first asked whether adenovirus-mediated gene transfer of anti-stathmin ribozyme would decrease the level of stathmin mRNA in murine breast cancer cells. Figure 2 shows northern blots of RNA isolated from uninfected cells or cells infected with either Ad.GFP or Ad.Rz184.GFP in different breast cancer cells. Cells transduced with the control Ad.GFP adenovirus show basal level of stathmin (lane 2) that is virtually similar to those of uninfected cells (lane 1) (Fig.2A & 2B). In contrast, SC115 cells transduced with Ad.Rz184.GFP showed a profound decrease (72.4%) in the level of stathmin mRNA (lane 3) (Fig.2A). Similarly, JC cells transduced with Ad.Rz184.GFP showed a 58% decrease in the level of stathmin mRNA (lane 3) (Fig.2B).

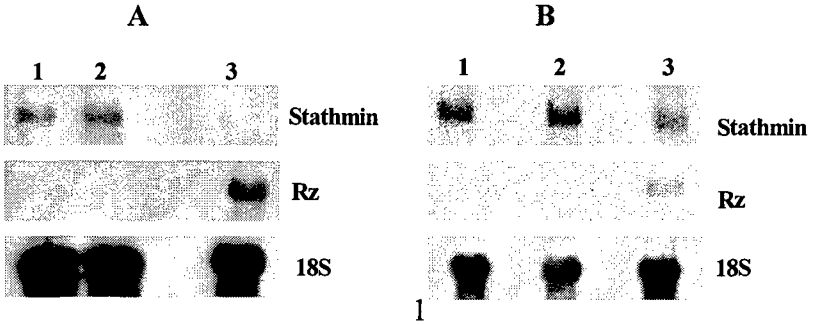

Fig. 2. Effects of anti-stathmin ribozyme on stathmin mRNA in murine breast cancer cells. (A) Northern blot of total RNA isolated from uninfected SC115 cells or SC115 cells infected with either Ad.GFP or Ad.Rz184.GFP at a moi of 100. (B) Northern blot of total RNA isolated from uninfected JC cells or JC cells infected with either Ad.GFP or Ad.Rz184.GFP at a moi of 200. Lanes 1, 2 and 3 represents 20 μgs of RNA isolated from uninfected cells, Ad.GFP infected cells and Ad.Rz184.GFP infected cells respectively. The filters were hybridized with stathmin, ribozyme & 18S probes as indicated.

The same filter was hybridized to a ribozyme probe to indicate ribozyme expression (Fig. 2). The level of stathmin mRNA was normalized to 18S ribosomal RNA to adjust for differences in RNA loading (Fig. 2). This experiment demonstrates that Ad.Rz184.GFP can efficiently downregulate stathmin mRNA levels in transduced breast cancer cells.

Effect of anti-stathmin ribozyme on the rate of proliferation:

We next examined the effects of the anti-stathmin ribozyme on the rate of proliferation of murine breast cancer cell lines. Fig. 3 illustrates the growth rates of uninfected cells or cells infected with the control Ad.GFP and the anti-stathmin Ad.Rz184.GFP adenovirus. When the cells were infected with Ad.GFP virus at different moi's, no significant growth inhibition was observed and the cells proliferated at the same rate as uninfected cells (Fig. 3A). In contrast, cells transduced with Ad.Rz184.GFP showed a dose-dependent growth inhibition, with essentially complete cessation of growth at an moi of 100 (Fig. 3B).

We also observed striking differences in the morphology of cells transduced with anti-stathmin adenovirus. A vast majority of the cells infected with anti-stathmin adenoviruses rounded up and detached from the culture dish after 3 to 4 days (data not shown). The rounding up and the detachment of cells in culture are typical of cells in mitosis that undergo profound cytoskeletal changes. Such morphological changes were not seen in cells infected with the control adenovirus, which remained as a monolayer.

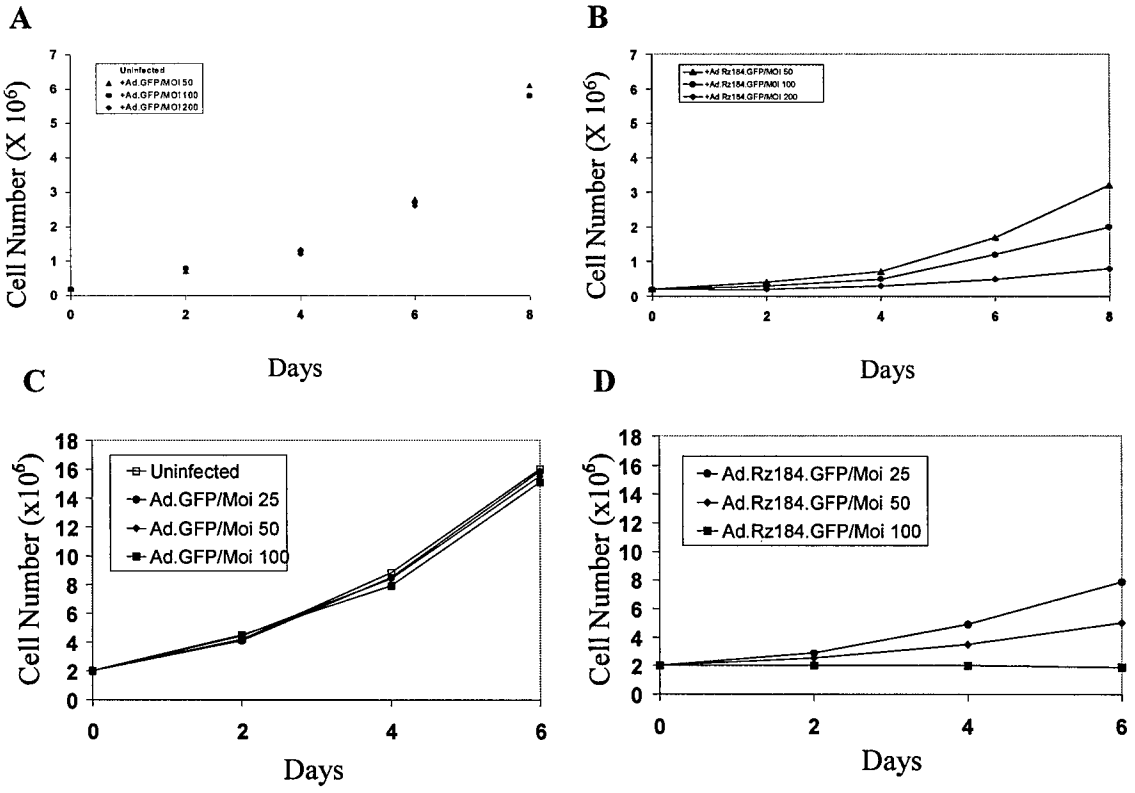

Fig. 3. Effects of anti-stathmin ribozymes on the rate of proliferation of murine breast cancer cell lines. (A) Growth curves of JC cells transduced with the control Ad.GFP adenovirus at different moi's as indicated. (B) Growth curves of JC cells transduced with Ad.Rz184.GFP anti-stathmin adenovirus at different moi's as indicated. (C) Growth curves of SC115 cells transduced with the control Ad.GFP adenovirus at different moi's as indicated. (D) Growth curves of SC115 cells transduced with Ad.Rz184.GFP anti-stathmin adenovirus at different moi's as indicated.

Effect of anti-stathmin ribozyme on cell cycle progression:

We also examined the effects of adenovirus-mediated transduction of anti-stathmin ribozyme on cell cycle progression of SC115 and JC breast cancer cells. Cells were infected with either control Ad.GFP or Ad.Rz184.GFP adenovirus at different moi's. After 48 hours, the cells were harvested, stained with propidium iodide and DNA content was assessed in a flow-cytometer. Representative DNA histograms are shown in figure 4. When JC or SC115 cells were transduced with the control Ad.GFP, no significant changes were seen in the DNA histogram relative to the uninfected cells (Fig. 4A & 4B). In contrast, cells transduced with Ad.Rz184.GFP showed a marked increase in the fraction of cells in the G2-M phases, with a corresponding decrease in the fraction of cells in the G0-G1 phases of the cell cycle (Fig. 4A & 4B). The accumulation of cells in the G2-M phases in the anti-stathmin adenovirus infected cells increased with increase in moi (data not shown).

To determine whether the observed differences in the DNA histograms may be a result of differences in the efficiency of viral transduction, we quantified the transduction efficiency by measuring the fraction of cells that express GFP. Small aliquots of cells from the experiment described above were fixed in 1% paraformaldehyde and analyzed for GFP fluorescence by flow cytometry. The fractions of transduced (i.e. GFP positive) cells were comparable in cells infected with Ad.GFP and Ad.Rz184.GFP (Fig. 4C & 4D). Thus, the observed differences in the cell cycle distribution of transduced cells are clearly not a result of differences in the efficiency of transduction. We also examined the spindle morphology of the infected cells by indirect immunofluorescence staining with an anti-tubulin antibody. Cell infected with the control Ad.GFP virus showed spindles with normal metaphase plates (Fig.4E). In contrast, cells infected with the Ad.Rz184.GFP showed spindle abnormalities with frequent multipolar spindles that had chromosomes aggregated in multiple metaphase plates (Fig.4F).

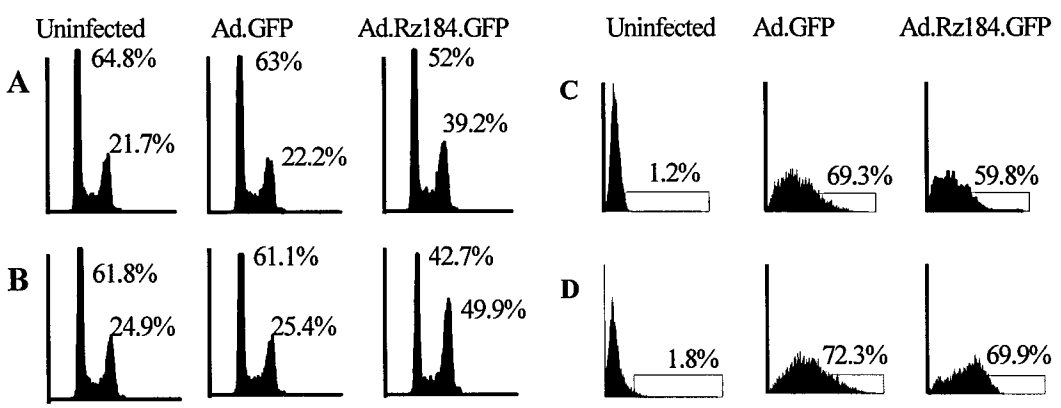

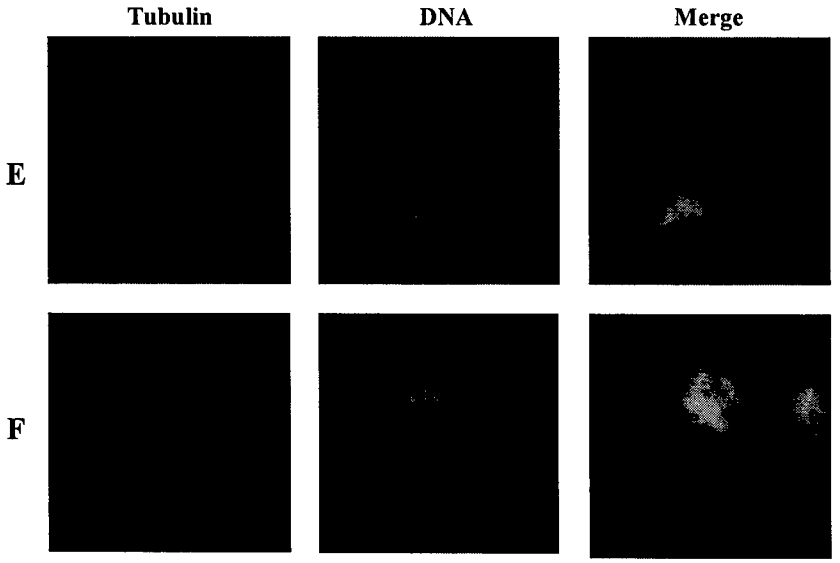

Fig. 4. Effects of anti-stathmin ribozymes on cell cycle progression. (A) DNA histograms of uninfected JC cells or JC cells infected with either Ad.GFP or Ad.Rz184.GFP as indicated. (B) DNA histograms of uninfected SC115 cells or cells infected with either Ad.GFP or Ad.Rz184.GFP as indicated. (C) GFP fluorescence analysis of uninfected JC cells or JC cells infected with either Ad.GFP or Ad.Rz184.GFP as indicated. (D) GFP fluorescence analysis of uninfected SC115 cells or SC115 cells infected with either Ad.GFP or Ad.Rz184.GFP as indicated. (E) Representative images of mitotic spindles in SC115 cells infected with control Ad.GFP. (F) Representative images of mitotic spindles in SC115 cells infected with Ad.Rz184.GFP. The photographs in the left panel show anti-tubulin staining, the middle panel shows DNA staining with DAPI and right panel shows an overlap of tubulin and DNA staining.

Effect of anti-stathmin ribozyme on clonogenicity:

We also studied the effects of anti-stathmin adenoviruses on the ability of JC and SC115 cells to form anchorage-independent colonies in semi-solid medium. Fig.5 illustrates the relative clonogenicity of uninfected cells and cells infected with either Ad.GFP or Ad.Rz184.GFP adenoviruses at different moi's. No significant differences in the clonogencity are seen when uninfected JC or SC115 cells are compared to the same cells infected with the control Ad.GFP adenovirus (Fig. 5A & 5B). In contrast, JC or SC115 cells infected with anti-stathmin adenovirus at different moi's show a dose-dependent inhibition of colony formation with a near complete suppression of anchorage independent growth. These results demonstrate that adenovirus mediated anti-stathmin ribozyme expression can inhibit tumorigenicity *in vitro*.

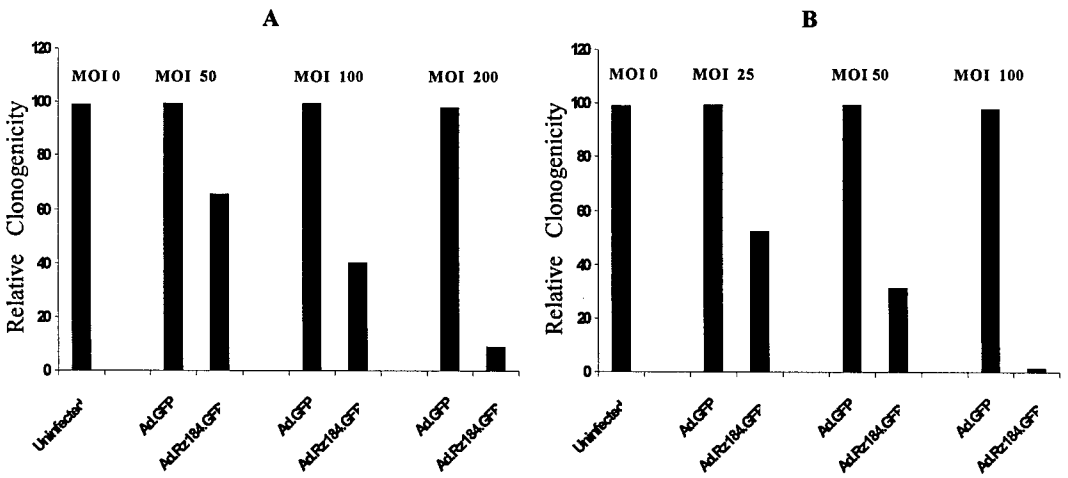

Fig. 5. Effects of anti-stathmin ribozymes on the clonogenicity. Equal number of cells were infected with either control or anti-stathmin adenoviruses at different moi's as indicated. After 3 hrs of infection, the virus was removed, the cells were washed in PBS and resuspended in 5 ml of methylcellulose based semisolid medium (0.9% methylcellulose, 1%BSA, and 0.1mM B-mercaptoethanol prepared in RPMI 1640 medium containing 30% fetal bovine serum, 100 units/ml penicillin, and 100 µg/ml streptomycin). The cells were then plated at a density of $1x10^4$ in 6-well tissue culture plates in triplicates and incubated at 37°C in 5% CO_2 atmosphere. The colonies that formed were counted at 2 weeks. (A) The bar graph illustrates the clonogenic potential of uninfected JC cells or JC cells infected with either Ad.GFP or Ad.Rz184.GFP at different moi as indicated. (B) The bar graph illustrates the clonogenic potential of uninfected SC115 cells or SC115 cells infected with either Ad.GFP or Ad.Rz184.GFP at different moi's as indicated. The relative clonogenicity of infected cells was calculated considering the clonogenic potential of uninfected cells as 100%.

Effects of anti-stathmin ribozyme on apoptosis:

In the experiments described above on the effects of anti-stathmin ribozyme expressing adenovirus on the growth of JC and SC115 cell lines, we had observed massive cell death approximately 5 days after infection with anti-stathmin adenovirus by trypan blue staining. Thus, we formally investigated the effects of the anti-stathmin recombinant adenovirus on apoptosis. We measured DNA fragmentation by anti-stathmin adenovirus using a TUNEL assay (Fig.6). Uninfected cells and cells infected with either Ad.GFP or Ad.Rz184.GFP were harvested on day 5, subjected to TUNEL reaction and analyzed by flow cytometry. When the cells were infected with control Ad.GFP virus, the fraction of TUNEL positive cells (2.9%) was very similar to that of uninfected cells (2.4%). In contrast, the fraction of TUNEL positive cells was significantly increased to 29% and 39% in Ad.Rz184.GFP infected JC and SC115 cells respectively (Fig.6A & 6B). Thus, these data confirm that ribozyme-mediated inhibition of stathmin expression can cause internucleosomal fragmentation of the genomic DNA.

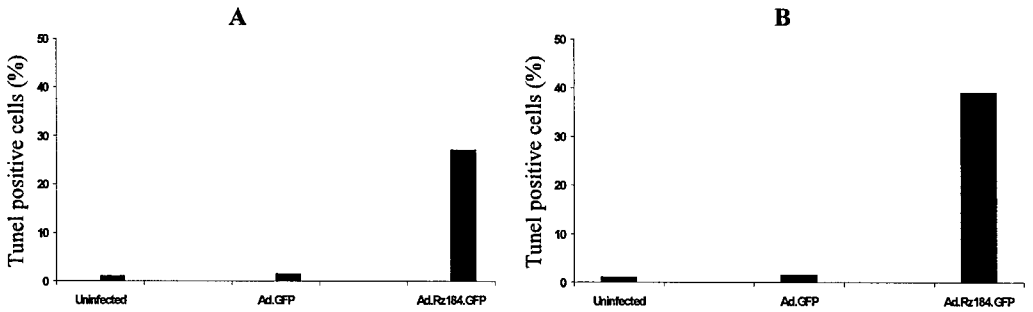

Fig. 6. Effects of anti-stathmin ribozymes on apoptosis. Equal number of cells were infected with either control Ad.GFP or Ad.Rz184.GFP at a moi of 100. The cells were harvested at day 5 and fixed in 2% Paraformaldehyde for 1 hr. The cells were then subjected to TUNEL (Terminal Deoxynucleotidyl transferase (TdT) mediated dUTP Nick End Labeling) assay. The fraction of TUNEL positive cells was assessed by flow cytometric analysis. (A) Bar graph illustrate the percentage of TUNEL positive cells in uninfected, Ad.GFP and Ad.Rz184.GFP infected JC cells as indicated. (A) Bar graph illustrate the percentage of TUNEL positive cells in uninfected, Ad.GFP and Ad.Rz184.GFP infected SC115 cells as indicated.

Effects of combination of taxol and anti-stathmin therapy *in vitro*:
We next examined whether the therapeutic effects of stathmin inhibition could be further enhanced by combining it with taxol, a chemotherapeutic drug that targets the mitotic spindle. We used three different assays to investigate the therapeutic interactions between taxol and anti-stathmin therapy. We evaluated the effects of combination of adenovirus mediated anti-stathmin therapy and taxol on proliferation, clonogenicity and apoptosis in breast cancer cells. For combination studies, we used low doses of the virus and the drug. The concentrations of taxol that we used were predetermined in pilot experiments and were below IC50. Fig.7 illustrates the effect of different concentrations of taxol on the rate of proliferation of JC cells in the presence and absence of anti-stathmin ribozyme therapy. Exposure of uninfected cells or cells infected with control Ad.GFP virus to different concentrations of taxol resulted in a very modest dose dependent decrease in growth. In contrast, exposure of cells infected with Ad.Rz184.GFP virus to the same concentration of drugs resulted in a very significant decrease in the rate of proliferation of cells.

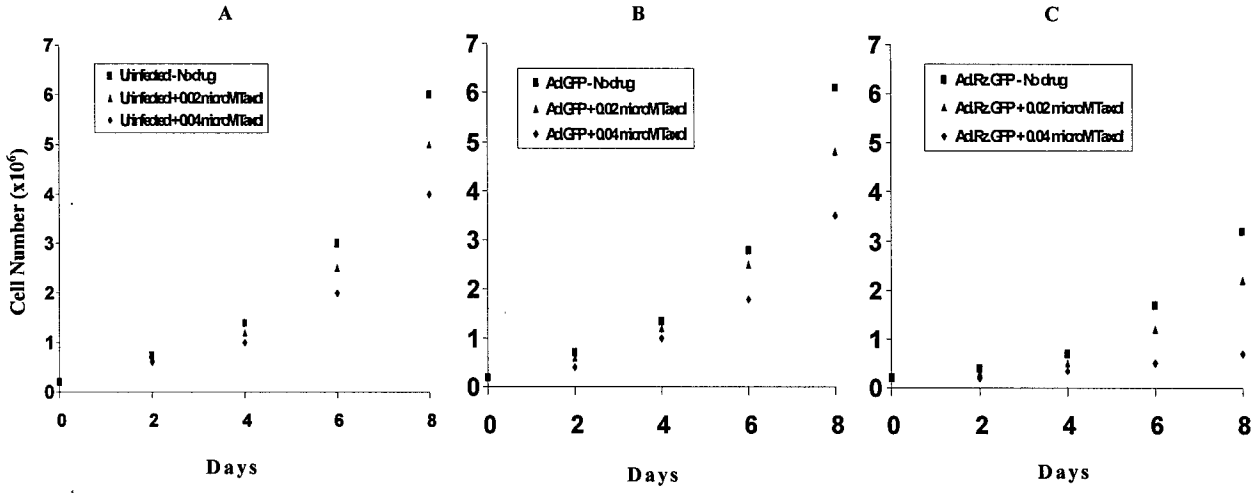

Fig.7 Effects of combination of taxol and anti-stathmin therapy on the rate of proliferation. Equal number of uninfected JC cells or JC cells infected with either control Ad.GFP or anti-stathmin Ad.Rz184.GFP viruses were exposed to taxol at the specified concentrations. Viable cells were counted on alternate days on a hemocytometer. (A) Growth curves of uninfected JC cells exposed to different concentrations of taxol. (B) Growth curves of Ad.GFP infected JC cells exposed to different concentrations of taxol. (C) Growth curves of Ad.Rz184.GFP infected JC cells exposed to different concentrations of taxol.

Interestingly, when the Ad.Rz184.GFP infected cells were exposed to higher concentration of taxol, there was a near complete loss of proliferation while the uninfected or control Ad.GFP infected cells exposed to the same dose of taxol continued to proliferate. In other words, stathmin-inhibition sensitized the cells to the growth inhibitory effects of taxol than uninfected cells or cells infected with the control virus.

We also examined the anti-tumor activities of combination of anti-stathmin therapy and taxol using *in vitro* clonogenic assays. Fig.8 illustrate the effects of combination of taxol and anti-stathmin therapy on the relative clonogenicity of uninfected cells and cells infected with either Ad.GFP or Ad.Rz184.GFP adenoviruses. Clonogenicity of the uninfected cells and cells infected with the control Ad.GFP virus was moderately reduced after exposure to increasing concentrations of taxol. In contrast, cells infected with Ad.Rz184.GFP showed a dose dependent inhibition of clonogenicity with a near complete loss of clonogenicity (1-2%) when the cells were exposed to taxol.

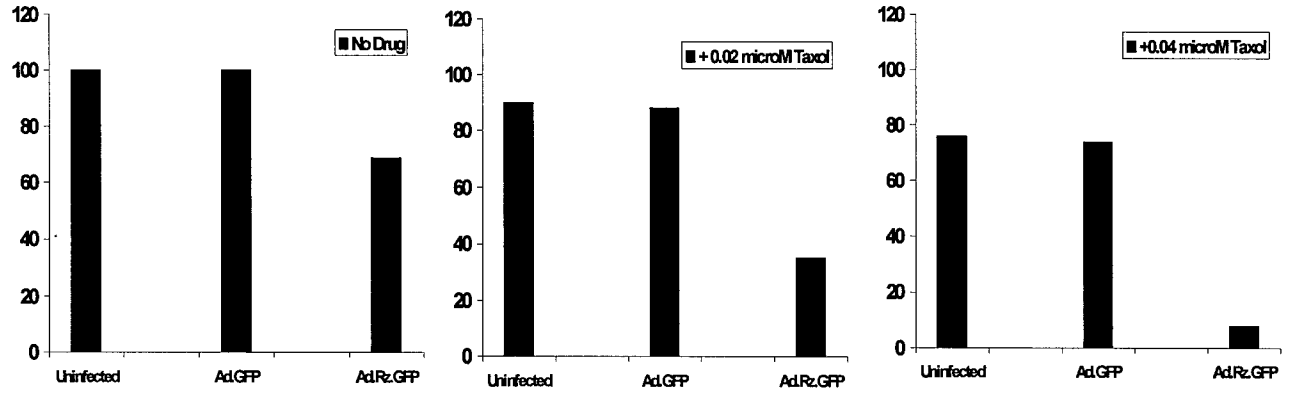

Fig.8 Effects of combinations of anti-stathmin therapy and taxol on the clonogenic potential JC cells. Equal number of cells were infected with either control or anti-stathmin adenoviruses at moi of 50. After 3 hrs of infection, the virus was removed and the cells were suspended in growth medium containing different concentrations of taxol as indicated. The cells were washed in PBS after 3 days and subjected to methylcellulose assay as described above. Bar graphs illustrate the relative clonogenicity of uninfected, control Ad.GFP and Ad.Rz184.GFP infected cells in the absence and presence of different concentrations of taxol as indicated.

We then analyzed the effects of combination of anti-stathmin therapy and taxol on the induction of apoptosis using TUNEL assay. Fig.9 illustrate the effects of combination of anti-stathmin therapy and taxol on apoptosis. TUNEL analysis of uninfected or control Ad.GFP infected cells showed modest apoptosis in the absence (0.4%) and presence (2.5-3.1%) of taxol. In contrast, cells infected with Ad.Rz184.GFP showed 3.5% TUNEL positive cells, which increased to 27.6% after exposure to taxol.

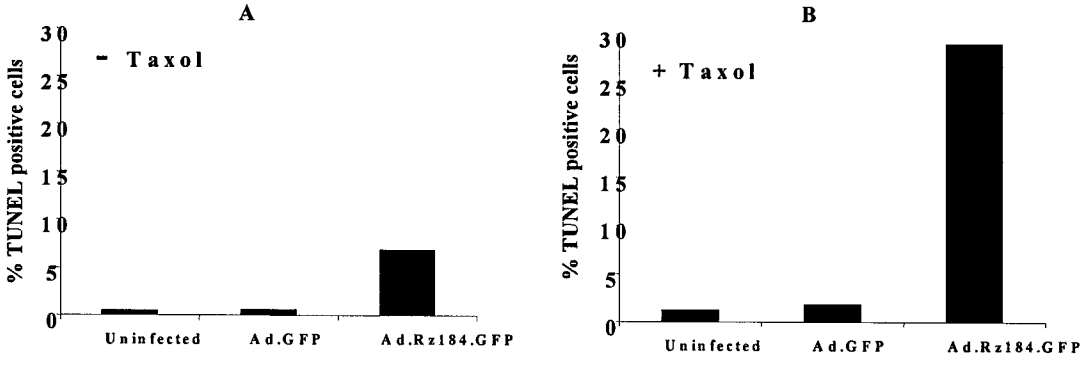

Fig.9 Effects of combination of taxol and anti-stathmin adenovirus on apoptosis. Equal number of uninfected JC cells and cells infected with either control Ad.GFP or Ad.Rz184.GFP were exposed to taxol for 5 days. The cells were then harvested, fixed in 2% paraformaldehyde and subjected to TUNEL (Terminal Deoxynucleotidyl transferase (TdT) mediated dUTP Nick End Labeling) assay. The fraction of TUNEL positive cells was assessed by flow cytometric analysis. (A) Bar graph showing the percentage of TUNEL positive cells in uninfected, Ad.GFP and Ad.Rz184.GFP infected cells in the absence of taxol as indicated. (B) Bar graph showing the percentage of TUNEL positive cells in uninfected, Ad.GFP and Ad.Rz184.GFP infected cells after exposure to taxol as indicated.

In all three assays that we used, the observed effects were much greater than the effects of either ribozyme alone or taxol alone. Overall, the effects of combination of anti-stathmin therapy with taxol were found to be clearly greater than the sum of their individual effects. This defines a synergistic interaction

between the two therapeutic modalities. Thus anti-stathmin therapy can markedly enhance the effects of taxol and can result in profound synergistic inhibition of proliferation, clonogenicity and apoptosis. Such a combination may provide a novel form of breast cancer therapy that would avoid the toxicities associated with the use of multiple chemotherapeutic agents.